

# Use of multiple extractions and injections to thermodynamically balance the humidification dehumidification desalination system

Karim M. Chehayeb<sup>a,\*</sup>, G. Prakash Narayan<sup>a,\*</sup>, Syed M. Zubair<sup>b</sup>, John H. Lienhard V<sup>a,\*\*</sup>

<sup>a</sup>*Department of Mechanical Engineering, Massachusetts Institute of Technology, Cambridge, MA 02139, USA.*

<sup>b</sup>*Department of Mechanical Engineering, King Fahd University of Petroleum and Minerals, Dhahran, Saudi Arabia.*

---

## Abstract

Humidification dehumidification (HDH) desalination systems are well suited for small scale, off-grid desalination. These systems are very robust and can tolerate a wide range of feed salinities, making them a good candidate for treating produced water from hydraulically fractured natural gas wells. A primary engineering challenge for these systems is their high thermal energy consumption. In this study, we examine the use of multiple air extractions and injections to thermodynamically balance the HDH system, so as to make it more energy efficient. The effect of the number of extractions on several performance parameters is studied. In addition, we study the effect of the enthalpy pinch, which is a measure of performance for a heat and mass exchanger, on these performance parameters. Finally, we present results that can be used as guidelines in designing HDH systems. These results include the identification of appropriate temperatures for the extracted/injected air streams, the division of the heat duty between stages, and the value of the mass flow rate ratio in each stage at various values of enthalpy pinch.

*Keywords:* desalination, humidification, dehumidification, thermodynamic balancing, enthalpy pinch, entropy generation minimization, mass extraction, heat and mass exchangers

---

---

\*Joint first authors

\*\*Corresponding author

*Email address:* lienhard@mit.edu (John H. Lienhard V)

## Nomenclature

### Acronyms

GOR	Gained Output Ratio (Eq. 17)
HDH	Humidification Dehumidification
HE	Heat Exchanger
HME	Heat and Mass Exchanger
RR	Recovery Ratio

### Symbols

$c_p$	specific heat capacity at constant pressure (J/kg·K)
$\dot{H}$	total enthalpy rate (W)
$g$	specific gibbs energy (J/kg)
$h$	specific enthalpy (J/kg)
$h^*$	specific enthalpy (J/kg dry air)
$h_{fg}$	specific enthalpy of vaporization (J/kg)
HCR	control volume based modified heat capacity rate ratio for HME devices (-)
$m_r$	water-to-air mass flow rate ratio (-)
$\dot{m}$	mass flow rate (kg/s)
$N$	number of extractions/injections (-)
$P$	absolute pressure (Pa)
$\dot{Q}$	heat transfer rate (W)
$s$	specific entropy (J/kg·K)
$sal$	feed water salinity (g/kg)
$\dot{S}_{gen}$	entropy generation rate (W/K)
$T$	temperature (°C)

### Greek

$\Delta$	difference or change
$\Psi$	enthalpy pinch (kJ/kg dry air)
$\phi$	relative humidity (-)
$\omega$	absolute humidity (kg water vapor per kg dry air)

### Subscripts

$a$	humid air
$c$	cold stream
$deh$	dehumidifier
$da$	dry air

<i>h</i>	hot stream
<i>hum</i>	humidifier
<i>HE</i>	heat exchanger
<i>i</i>	stage number
<i>in</i>	entering
<i>int</i>	water-vapor interface
<i>max</i>	maximum
<i>loc</i>	defined locally
<i>out</i>	leaving
<i>pw</i>	pure water
<i>rev</i>	reversible
<i>tot</i>	total
<i>w</i>	seawater

## 1. Introduction

Humidification dehumidification (HDH) is a distillation technology which imitates the rain cycle in a controlled fashion by using a carrier gas, such as air [1–3], to transport water vapor between different compartments. The most basic system consists of a humidifier, a dehumidifier, and a heater. As shown in Fig. 1, cold air enters the humidifier where it is directly exposed to a hot stream of saline water, so its temperature increases, thus increasing its capacity to hold water vapor. Water from the saline water stream thus evaporates, making the air stream more humid. The humid air is then taken to the dehumidifier, where it is put in indirect contact with the cold incoming saline water stream. The temperature of the air decreases, causing some of the water vapor to condense, thus supplying a stream of pure water.

[Fig. 1 about here.]

HDH is a promising technology for small scale desalination and is appropriate for water production in remote, off-grid locations where the water demand is not large enough to justify installing large scale plants. In addition, HDH systems do not require very sophisticated components and maintenance. Furthermore, HDH is a very robust technology, which, unlike membrane based technologies, can treat very saline water (many times saltier than seawater), which makes it a strong candidate for addressing the problem of produced water from natural gas wells. The major limitation of this technology is its high energy consumption. However, the energy requirements can be reduced through a careful understanding of the thermodynamics underpinning this technology so as to reduce the entropy generation within the operating cycle [4–6]. It has been shown previously that the entropy production rate is at a minimum when the heat capacity rates of the interacting streams in a heat and mass exchanger are equal [7]. This thermodynamically balanced system can be achieved through the variation of the mass flow rate ratio of the interacting streams (namely water and air) in each of the humidifier and dehumidifier which may be attained by mass extraction and

injection between the two components at one or more internal locations [2]. In this study, we consider air extractions from the humidifier to the dehumidifier as shown in Fig. 1.

### 1.1. Literature review

Previous attempts to increase the energy efficiency of HDH desalination systems using mass extraction/injection have been reported in the literature. Müller-Holst [8, 9] suggested that entropy generation is minimized when the stream-to-stream temperature difference is kept constant throughout the system. In that study, it was proposed that a constant temperature pinch could be achieved by continuously adjusting the water and dry air volume flow rates. In addition, that study reported an optimized energy consumption of around 430 kJ/kg.

Zamen et al. [10] proposed using a multi-stage process, where the water-to-air mass flow rate would be varied between stages. A temperature pinch was used to define the performance of the system, and the model got up to four stages. It was reported that a two-stage system was the best configuration with the tested system since additional stages would not result in a substantial increase in efficiency. For a four-stage system with a temperature pinch of 4°C, operating between 20 °C and 70 °C, the heat input was around 800 kJ/kg. Similarly, Hou et al. [11] modeled a 2-stage system, and reported an energy recovery ratio of 0.836 at a temperature pinch of 1 °C.

McGovern et al. [12] studied the variation of the energy efficiency (represented by the gained output ratio, or GOR) and the recovery ratio with varying temperature pinch. The study reported an increase in GOR from 3.5 in a system with no extraction to 14 in a system with a single water extraction at effectively infinite heat and mass exchanger area with both systems at a feed temperature of 25 °C and a top moist air temperature of 70 °C. In addition, the recovery ratio increased from 7 % to 11 % with a single water extraction under the same conditions.

Thiel and Lienhard [13] suggested that in a heat and mass exchanger involving high concentrations of noncondensable gases, which is the case of the dehumidifier in any HDH

system, the entropy generation is mainly due to mass transfer, and a balanced system is closer to a balanced humidity profile than a balanced temperature profile.

Narayan et al. [14] defined an enthalpy pinch, and used it in balancing devices with combined heat and mass transfer since a temperature pinch alone does not take the mass transfer into account. This parameter was used in defining balanced systems with no extraction, single extraction, and infinite extractions. In a subsequent experimental study, Narayan et al. [15] increased the GOR from 2.6 to 4.0 using a single air extraction with a system having an enthalpy pinch of 19 kJ/kg of dry air operating between 25 °C and 90 °C.

### *1.2. Goals of the current study*

This study complements the previous paper by Narayan et al. [14]. We examine the effect of a finite number of extractions on energy efficiency, water recovery, and total heat duty. We also aim to understand when it is useful to use extractions and injections, and how many should be used for systems of different size. Additionally, we present results that can be used in designing HDH systems, including the division of the heat duty between stages, the mass flow rate ratio in each stage, and the temperatures of the extracted/injected air streams.

## **2. Modeling**

### *2.1. Definition of a balanced system*

Previous studies by Narayan et al. [7, 16] concluded that entropy generation is minimized at a fixed energy effectiveness when the modified heat capacity rate ratio (HCR) in the dehumidifier is equal to unity, where:

$$\text{HCR} = \frac{\Delta\dot{H}_{\text{max,cold}}}{\Delta\dot{H}_{\text{max,hot}}} \quad (1)$$

[Fig. 2 about here.]

In Eq. 1, the numerator and denominator can both be divided by the mass flow rate of dry air, and, as shown in Fig. 2, the resulting equation can be written as follows:

$$\text{HCR} = \frac{\Delta h_{\max, \text{cold}}^*}{\Delta h_{\max, \text{hot}}^*} = \frac{\Delta h^* + \Psi_{\text{deh, cold}}}{\Delta h^* + \Psi_{\text{deh, hot}}} \quad (2)$$

where  $\Psi$  is the enthalpy pinch [14], which may be thought of as the minimum loss of enthalpy rate due to a finite device size. For HCR to be equal to unity in the dehumidifier, we need  $\Psi_{\text{deh, cold}} = \Psi_{\text{deh, hot}}$ . This means that in a balanced HDH system the enthalpy pinch point will be located at the inlet and outlet of the dehumidifier, and at a single intermediate location in the humidifier. The same definition is used for a system with multiple extractions and injections, where each stage (between two consecutive extraction or injection points) satisfies these conditions.

## 2.2. Conservation equations and solution method

As explained in previous publications [12, 14], the HDH system can be modeled using temperature-enthalpy diagrams. These diagrams allow the representation of the process paths followed by each of the interacting streams, namely, moist air and seawater in the humidifier, and moist air, seawater, and distillate in the dehumidifier. Having the process paths defined allows the calculation of the enthalpy pinch at any location in the heat and mass exchangers. The enthalpy in these diagrams is expressed in kJ per kg of dry air since normalizing it in this fashion, as suggested by McGovern et al. [12], allows the representation of the process paths of air and water on the same diagram, and inherently satisfies the energy balance as will be shown in this section. The air, assumed to be saturated at all times, follows the air saturation curve, where the enthalpy is only a function of temperature.

[Fig. 3 about here.]

Figure 3 shows a control volume containing the heater and portions of the humidifier and the dehumidifier. The control volume is chosen such that it intersects the humidifier and the

dehumidifier in a location where the air is at the same temperature and mass flow rate in both components. The intersection of the control volume with both components corresponds to a vertical line (constant specific enthalpy of dry air) on the temperature-enthalpy profile. The water content in the air entering the control volume in the humidifier is the same as that in the air exiting the control volume in the dehumidifier since the air is saturated and at the same temperature. A water mass balance on this control volume results in

$$\dot{m}_{w,hum} = \dot{m}_{w,deh} - \dot{m}_{pw,loc} \quad (3)$$

where the “loc” subscript denotes that the mass flow rate indicated is that of pure water condensed starting from the hot end of the dehumidifier up to the location in question. Note that, in the dehumidifier, the saline water is not in contact with the air so its mass flow rate is constant throughout the dehumidifier, and the saline water that enters the heater and the humidifier has the same mass flow rate as the feed saline water,  $\dot{m}_w$ . So at any location in the humidifier,

$$\dot{m}_{w,hum} = \dot{m}_w - \dot{m}_{pw,loc} \quad (4)$$

A more intuitive way to look at this result is that, at any location in the humidifier, the mass flow rate of saline water is the mass flow rate of water at the inlet of the humidifier minus the amount of water that has evaporated up to this location.

[Fig. 4 about here.]

Figure 4(a) represents a control volume containing a small section of the dehumidifier. A water mass balance on this control volume results in

$$\dot{m}_{pw,1} - \dot{m}_{pw,2} = \dot{m}_{da} (\omega_2 - \omega_1) \quad (5)$$



In addition, an energy balance on the same control volume can be expressed as

$$\left(\dot{H}_2 - \dot{H}_1\right)_w - \left(\dot{H}_2 - \dot{H}_1\right)_{pw} = \left(\dot{H}_2 - \dot{H}_1\right)_a \quad (6)$$

or

$$\dot{m}_w c_{p,w} (T_2 - T_1)_w - \left[ (\dot{m} c_p T)_{pw,2} - (\dot{m} c_p T)_{pw,1} \right] = \dot{m}_{da} (h_2^* - h_1^*) \quad (7)$$

For an infinitesimally small control volume, the change in the enthalpy rate of pure water is mainly due to temperature change, so the change in mass flow rate of pure water inside the control volume can be neglected, such that  $\dot{m}_{pw,2} = \dot{m}_{pw,1} = \dot{m}_{pw,loc}$ . Assuming that, at any location in the dehumidifier, the condensed water is at the same temperature as the saline water, and that the specific heat capacity of water is constant and the same for pure water and saline water, the energy balance simplifies to

$$(\dot{m}_w - \dot{m}_{pw,loc}) c_{p,w} (T_2 - T_1)_w = \dot{m}_{da} (h_2^* - h_1^*) \quad (8)$$

Dividing Eq. 8 by the product  $(\dot{m}_w - \dot{m}_{pw,loc}) c_{p,w} (h_2^* - h_1^*)$ , and taking the limit as  $(h_2^* - h_1^*)$  goes to zero, we obtain the following expression for the slope of the process path followed by the water stream in the dehumidifier on the temperature-enthalpy diagram:

$$\frac{dT_w}{dh^*} = \frac{1}{m_r c_{p,w}} \quad (9)$$

where the mass flow rate ratio,  $m_r$ , is the ratio of the net mass flow rate of water to that of dry air:

$$m_r = \frac{\dot{m}_w - \dot{m}_{pw,loc}}{\dot{m}_{da}} \quad (10)$$

Similarly, an energy balance can be applied on the humidifier control volume shown in Fig. 4(b), and can be combined with Eq. 4 to give

$$\left(\dot{H}_2 - \dot{H}_1\right)_w = \left(\dot{H}_2 - \dot{H}_1\right)_a \quad (11)$$

and

$$(\dot{m}_w - \dot{m}_{pw,loc}) c_{p,w} (T_2 - T_1)_w = \dot{m}_{da} (h_2^* - h_1^*) \quad (12)$$

The resulting equation is the same as Eq. 8, which indicates that the slope of the process path of water in the humidifier is also given by Eq. 9, and, on the temperature-enthalpy diagrams, the humidifier and dehumidifier lines should always be parallel. As a result of Eq. 9, varying the mass flow rate ratio through extractions of air from the humidifier to the dehumidifier allows the modification of the slope of the water process paths on the temperature-enthalpy diagram, and hence allows the balancing of the heat and mass exchangers.

In the present paper, the boundary conditions used in all simulations are a feed water temperature of 20 °C and a top brine temperature of 80 °C. The primary independent variables are the number of extractions,  $N$ , and the enthalpy pinch,  $\Psi$ . The algorithm used in this study is presented in the form of a flowchart in Fig. 15 in the Appendix. The first part of the calculations is purely numerical and consists of finding the correct temperatures of the extracted/injected air streams that yield a balanced system, as defined in Section 2.1. After finding the appropriate temperature-enthalpy profile for a given  $N$  and  $\Psi$ , we can calculate all the parameters needed to evaluate the performance of the system. A typical balanced temperature-enthalpy profile is shown in Fig. 5, where  $N = 3$  and  $\Psi = 3$  kJ/kg dry air.

[Fig. 5 about here.]

Equation 9 can be rearranged to calculate the mass flow rate ratio in the final stage of the system:

$$m_r = \frac{1}{\frac{dT_w}{dh^*} \times c_{p,w}} \quad (13)$$

As explained in Sections 2.3 and 3.2, the mass flow rate ratio is assumed constant in each stage. In addition, at the hot end of the dehumidifier,  $\dot{m}_{pw,loc} = 0$  kg/s so the mass flow rate of dry air in the final stage can be calculated using Eq. 10. Given  $\dot{m}_{da,N+1}$ , the amount of pure water produced in the final stage can be calculated:

$$\dot{m}_{pw,N+1} = \dot{m}_{da,N+1} \Delta\omega_{N+1} \quad (14)$$

Equation 13 can then be used to calculate the mass flow rate ratio in the  $N^{th}$  stage, and, having calculated  $\dot{m}_{pw,N+1}$ , which is the local mass flow rate of pure water at the inlet of the  $N^{th}$  stage,  $\dot{m}_{da,N}$  can be calculated using Eq. 10. The same procedure can be repeated to find the mass flow rate of dry air in each stage.

Additionally, the total mass flow rate of product water can be calculated:

$$\dot{m}_{pw,tot} = \sum_{stage,i=1}^{N+1} \dot{m}_{da,i} \Delta\omega_i \quad (15)$$

Finally, the total heat input into the system is calculated by applying the First Law of Thermodynamics on the heater:

$$\dot{Q}_{in} = \dot{m}_w \Delta h_w \quad (16)$$

### 2.3. Assumptions and approximations

- Specific heat capacity of water is assumed constant, evaluated at 50 °C, and a salinity of 35 ppt (maximum actual variation < 5 %)
- Temperature-enthalpy data for saturated air is input into the MATLAB code in the form of an array with a finite difference between consecutive data points. The discretization of the database is small enough such that the resulting uncertainty is reasonably small ( $\ll 1$  %)
- In the dehumidifier, pure water is produced at the temperature of seawater at the corresponding location. This means that pure water and seawater follow the same

process path in the dehumidifier. The maximum error resulting from this assumption is small ( $< 2\%$ ) and is discussed in an earlier publication [14].

- Air is assumed to be always saturated, which means the process path of air on the temperature-enthalpy diagrams is the same as the air saturation curve (discussed in previous publications, and shown to have an uncertainty  $< 10\%$  [12, 14])
- An additional assumption to further simplify the modeling procedure of multiple extractions/injections is that of a constant mass flow rate ratio in each stage. This is discussed in detail in Section 3.2 of the present study.

#### 2.4. Performance parameters

In order to assess the performance of an HDH system, we need to first evaluate its energy efficiency. A common parameter used in thermal desalination systems is the Gained Output Ratio, or GOR, which is the ratio of the latent heat of vaporization of the product water to the net heat input to the system:

$$\text{GOR} = \frac{\dot{m}_{pw} h_{fg}}{Q_{in}} \quad (17)$$

GOR is a dimensionless quantity which measures the extent of reuse of the heat input. The most basic distillation system that uses heat to directly boil water without recovery of the heat of condensation would have at most a GOR of 1. In the present study,  $h_{fg}$  is taken constant and equal to 2400 kJ/kg.

Another parameter of interest is the Recovery Ratio, RR. It is defined as the amount of pure water produced per unit amount of feed entering the system.

$$\text{RR} = \frac{\dot{m}_{pw}}{\dot{m}_w} \quad (18)$$

A third parameter used in this study is the heat duty, which is the total energy transfer between the interacting streams summed over all stages of a single component type (humid-

ifiers or dehumidifiers) per unit amount of water produced.

$$\dot{Q}_{\text{duty}} = \frac{\sum_{\text{stage}, i=1}^{N+1} \dot{m}_{da,i} \Delta h^*_i}{\dot{m}_{pw}} \quad (19)$$

In a closed-air system, such as the one studied here, the heat duty is the same in both the humidifier and the dehumidifier. The heat duty, along with the driving force (e.g. temperature difference for a heat exchanger), determines the size of the heat and mass exchangers [17]. Therefore, at a constant enthalpy pinch, the heat duty can be used as a rough indicator of the initial cost of the system. It should be noted that the heat duty is different from (and larger than) the heat input,  $\dot{Q}_{in}$ .

### 2.5. Property packages

- The thermophysical properties of seawater were evaluated using the correlations developed by Sharqawy et al. [18].
- Thermophysical properties of pure water are evaluated using the IAPWS (International Association for Properties of Water and Steam) 1995 Formulation [19].
- Moist air properties are evaluated assuming an ideal mixture of air and steam using the formulations of Hyland and Wexler [20].

Moist air properties thus calculated are in close agreement with the data presented in ASHRAE Fundamentals [21] and pure water properties are equivalent to those found in NIST's property package, REFPROP [22].

## 3. Results and Discussion

### 3.1. Experimental validation

In a recent study, Narayan et al. [15] built an HDH system having an enthalpy pinch of 19 kJ/kg dry air at optimal operation. The GOR of the system without any extractions was 2.6, and that of a system with a single extraction/injection was 4.0. The system described

in that study operated between 25 °C and 90 °C and had an uncertainty of  $\pm 5\%$  on GOR. Performing the numerical calculations at these boundary conditions and at  $\Psi = 19$  kJ/kg dry air, the calculated GOR was 2.3 for the case of no extraction (11 % difference) and 4.7 for that of a single extraction (17 % difference). The deviation of the experimental results from the numerical results presented in this paper is expected since the experimental setup had some heat losses to the environment. The experimental system also had additional entropy generation due to mixing when injecting the air stream into the dehumidifier, and the ambient conditions could have varied slightly. In addition, the numerical study uses some simplifying assumptions, as explained in Section 2.3, which leads to a small error in the values of GOR. Nonetheless, the reported results are reasonably close to the experimental results, and serve the main purpose of showing trends in the variation of the different performance parameters with varying enthalpy pinch and number of extractions/injections.

### *3.2. Effect of assuming fixed mass flow rate ratio*

In the results reported in the following sections, the mass flow rate ratio, defined in Eq. 10, is kept constant in each stage of both the humidifier and the dehumidifier. This results from the assumption that the water flow rate is kept constant in each of these components. In other words, the effect of condensation on the flow rate of water in a dehumidifier stage and evaporation in the corresponding humidifier stage can be neglected since the mass flow rate of the condensed or evaporated water is very small compared to that of the mass flow rate of saline water. This approximation, along with that of a constant specific heat capacity of water, translates into a constant slope (Eq. 9), so the process path of water in each stage will be a straight line, making the numerical computation much simpler and faster.

In order to estimate the error caused by this approximation, additional calculations were done in which the mass flow rate ratio was actually varied to account for condensation and evaporation for the cases of no extraction and single extraction. The maximum error on the gained output ratio, GOR, was found to be around 1 % for the case of no extraction [Fig. 6(a)], and 2.5 % for that of single extraction [Fig. 6(b)]. As will be shown in Section 3.5,

the recovery ratio converges to a maximum, and, after the first extraction, the increase in recovery ratio is limited. This, in turn, means that the error due to the assumption of constant mass flow rate ratio within each stage will not increase significantly for a higher number of extractions since condensation and evaporation are bounded by the total recovery.

[Fig. 6 about here.]

### 3.3. Temperature of the extracted streams

As explained in Section 2.2, the appropriate temperatures of the extracted/injected air streams are determined by using a purely numerical approach. The correct temperature-enthalpy profile is the one that leads to a thermodynamically balanced system as defined in Section 2.1. Figure 7 presents the appropriate temperatures of the extracted/injected air streams at various  $\Psi$  and  $N \leq 5$ . Starting with  $N = 5$  at  $\Psi = 0$  kJ/kg dry air, it can be seen that, as the enthalpy pinch increases, the appropriate temperature of extraction/injection decreases. That is, if we have 5 extractions/injections (and therefore six balanced stages), as  $\Psi$  increases, the required temperature of each of these extractions/injections will decrease. A limiting enthalpy pinch for  $N = 5$  is reached when the temperature of the first extraction point becomes equal to that of the air at the humidifier inlet (at  $\Psi \approx 3.5$  kJ/kg dry air). In other words, the first extraction becomes redundant, thus reducing the number of effective extractions to  $N = 4$  and the number of stages to five balanced stages. Similarly, at  $\Psi \approx 8$  kJ/kg dry air, for a three extraction system, the first of the three extractions occurs at the temperature of the inlet, so we are reduced to 2 useful extractions that yield three balanced stages. What can be concluded from this graph is that at any enthalpy pinch there is only a limited number of extractions/injections that can yield a fully balanced system. A higher number of extractions for that enthalpy pinch would cause imbalance in the system, as well as raise capital cost. Therefore, for the boundary conditions studied, Fig. 7 presents the optimal temperatures of extraction/injection at any given enthalpy pinch for  $N \leq 5$ . Note that, at an enthalpy pinch higher than 35 kJ/kg dry air, the performance of the system does

not improve if we extract/inject even once since the balanced system would be composed of a single balanced stage, which can be implemented simply by choosing the correct mass flow rate ratio (discussed in Section 3.8).

[Fig. 7 about here.]

This brings us to the idea of continuous balancing proposed in an earlier publication [14], specifically using an infinite number of infinitesimal extractions/injections. It is now better understood why a continuously balanced component could be less efficient than a balanced system without any extractions/injections. In the model proposed for continuous extraction, only one component could be balanced at finite area. So as the enthalpy pinch increases we could have large entropy production rates in the “unbalanced” component, thus reducing the efficiency of the system. In the case of a finite number of extractions, both components of the system are balanced in each stage as explained in Section 2.1. Continuous extraction is therefore only beneficial at infinite heat and mass exchanger surface area, i.e. at  $\Psi = 0$  kJ/kg dry air.

Figure 8 presents the variation of the temperature of extraction/injection with  $N$  at infinite area. Since the approach used in this study is numerical, getting the initial guess value of the location of the extraction to be the closest possible to the correct value is critical in reducing the computing time. So, if the temperature of an extraction is known for the case of  $N$  extractions at a given enthalpy pinch, Fig. 8 shows that the temperature of the same extraction at  $N + 1$  extractions will be lower.

[Fig. 8 about here.]

#### *3.4. Variation of GOR with enthalpy pinch and number of extractions*

The variation of GOR with  $N$  and  $\Psi$ , presented in Fig. 9, can best be explained by looking back at the variation of the temperature of extractions with  $\Psi$  in Fig. 7. It can be seen that the variation of the temperature of the extractions is smooth with varying enthalpy pinch. So when the transition enthalpy pinch is reached, and the number of extractions



is decreased by one, the temperature profile of the system does not vary much. In other words, when the optimal location of the first extraction becomes the inlet of the humidifier, the number of extractions is reduced by one while the temperature of the other extraction points is only varied slightly. For example, when the maximum number of extractions goes from 3 to 2 at  $\Psi \approx 8$  kJ/kg dry air, the 2nd and 3rd extractions remain at almost the same temperature. So the temperature profile of a system with three extractions at an enthalpy pinch just smaller than the transition enthalpy pinch will be the same as that of a system with two extractions at an enthalpy pinch just larger than the transition pinch. This means that the characteristics of these systems will be very close, which explains why the curves of GOR at various  $N$  intersect. Thus, at the transition enthalpy pinch between  $N$  and  $N + 1$  extractions, the system with  $N$  extractions and that with  $N + 1$  extractions have the same GOR, among other parameters, namely RR, heat duty, and mass flow rate ratio in each stage.

As expected, at a constant  $N$ , GOR decreases with increasing  $\Psi$ . This is true since the difference in both, temperature and humidity, is larger at larger  $\Psi$ , which means that the entropy generation is greater, and the energy efficiency is smaller. In addition, at a constant  $\Psi$ , the GOR is greater at a larger number of extractions since the process paths of the interacting streams become closer, and the driving forces for the heat and mass transfer become smaller, reducing the entropy generation and increasing the energy efficiency.

Another observation from Fig. 9 is that the effect of extracting is largest at infinite area where each additional extraction increases the efficiency by a significant amount. The larger the enthalpy pinch, the smaller the effect of additional extractions/injections. Also, when the enthalpy pinch is greater than 6 kJ/kg dry air, we notice that extractions/injections have diminishing returns as suggested by Zamen et al. [10]. That is, the increase in efficiency due an additional extraction is smaller than the increase due the previous extraction. For example, at  $\Psi = 7$  kJ/kg dry air, the first extraction improves GOR by 3.9, the second by 3.6, and the third by 1.2. This observation is not true for  $\Psi \leq 6$  kJ/kg dry air where each

additional extraction brings a significant increase in efficiency, in some cases even greater than that due to the previous extraction.

[Fig. 9 about here.]

### 3.5. Variation of Recovery Ratio with enthalpy pinch and number of extractions

As can be seen in Fig. 10, for the same number of extractions/injections, the recovery ratio decreases with increasing enthalpy pinch, and, as was explained in Section 3.4, the recovery ratio of  $N + 1$  extractions intersects that of  $N$  extractions at the transition enthalpy pinch. The recovery ratio increases with the number of extractions/injections; however, this increase becomes smaller with each additional extraction/injection. For a closed-air, open-water (CAOW) system operating between 20 °C and 80 °C, and balanced using air extractions/injections, the recovery ratio converges to a limit close to 7.6 % at infinite area as  $N$  goes to infinity.

When comparing Fig. 10 to Fig. 9, we notice that balancing through air extractions and injections has a much larger effect on energy efficiency than on recovery ratio.

[Fig. 10 about here.]

### 3.6. Variation of heat duty with enthalpy pinch and number of extractions

The variation of heat duty with  $N$  and  $\Psi$ , shown in Fig. 11, is similar to that of recovery ratio. The total heat duty decreases with increasing enthalpy pinch. Also, the heat duty increases with the number of extractions/injections until it reaches a limit of about 3050 kJ/kg of distillate for our boundary conditions at infinite area. It can be seen that the variation of the heat duty at  $N \geq 3$  at  $\Psi$  close to 0 is not very smooth, but we should note that the variation is between 3020 and 3050 kJ/kg of distillate, which is less than 1 %, and falls within the numerical error range.

An important observation to be made is that a small increase in heat duty can lead to a large increase in GOR. For example, at  $\Psi = 15$  kJ/kg dry air, the first extraction will

double the GOR while only needing a 4 % increase in heat duty, which suggests a significant increase in performance at only a modest increase in system cost. As noted in Section 3.4, GOR increases faster with  $N$  at  $\Psi$  close to 0, whereas the variation of heat duty with  $N$  becomes very small in that region. This means that the additional efficiency comes at a cheap price if we can achieve a low enthalpy pinch at an acceptable cost.

[Fig. 11 about here.]

### 3.7. Division of heat duty between stages

The data presented in this section could be considered as a guideline in designing an HDH system. Figure 12(a) presents the division of the total heat duty between the different stages of the system at infinite area (which corresponds to  $\Psi = 0$  kJ/kg dry air). As a rough estimate, the heat duty is almost divided equally between the different stages. The farther the system is from infinite area, the less uniform the division of the heat duty at high  $N$ , as shown in Fig. 12(b).

[Fig. 12 about here.]

The same results can be seen in Fig. 13, which presents the optimal division of heat duty between stages for various values of enthalpy pinch. This means that the cases presented show the maximum number of extractions possible at any given  $\Psi$  (where  $N \leq 5$ ). Starting with six stages at  $\Psi = 0$  kJ/kg dry air, the heat duty is almost divided equally between stages. As  $\Psi$  increases, the fraction of the heat duty in the first stage decreases before reaching 0 at the transition enthalpy pinch, and thus the number of extractions/injections is reduced by 1.

[Fig. 13 about here.]

### 3.8. Optimal values for mass flow rate ratio for varying enthalpy pinch

Figure 14 shows the optimal value of the mass flow rate ratio in each stage at various values of enthalpy pinch. As expected, the mass flow rate ratio is always higher in the hotter stages since we are extracting air from the humidifier and injecting it in the dehumidifier. So

there is more air at the lower stages, and hence a lower mass flow rate ratio. In addition, the mass flow rate ratio decreases in each stage with increasing enthalpy pinch until a minimum  $m_r$  of around 1 is reached in the first stage at the transition enthalpy pinch. After some investigation, it was found that the mass flow rate ratio is close to 1 due the boundary condition  $T_{feed} = 20$  °C since in that region  $\frac{dT_a}{dh^*} \approx c_{p,w}$ .

[Fig. 14 about here.]

#### 4. Conclusions

The effect of the number of extractions and the enthalpy pinch on various performance parameters of a closed-air, open-water humidification dehumidification system has been studied. The main conclusions of this work are the following:

1. At a given enthalpy pinch, we can only extract/inject beneficially a limited number of times.
2. Continuous extraction, as proposed in an earlier publication [14], can only fully balance one component. Therefore, at a given enthalpy pinch, continuous extraction can be less beneficial than a finite number of extractions, which is able to balance both components.
3. Recovery ratio converges to a maximum as the number of extractions/injections increases.
4. Total heat duty converges to a maximum as the number of extractions/injections increases.
5. When modeling closed-air, open-water HDH systems with air extractions/injections, the change in mass flow rate ratio due to evaporation/condensation within a stage can be neglected.
6. A small increase in heat duty can lead to a large increase in energy efficiency, especially at a small enthalpy pinch.
7. The effect of balancing through extraction/injection is greater at smaller enthalpy pinch, where GOR increases faster with  $N$  and heat duty remains approximately con-

stant. At larger enthalpy pinch (smaller heat and mass transfer surface area), balancing has diminishing returns.

8. Location of the injection points:

a) As the enthalpy pinch increases, the optimal temperature of the extracted/injected air stream decreases.

b) As the number of extractions/injections increases, the optimal temperature of the extracted/injected air stream decreases.

9. Balancing has a much smaller effect on recovery ratio than on energy efficiency.

In addition, this study presents results that can be used in designing HDH systems. These results include the optimal temperatures of the extractions/injections, the division of the heat duty between stages, and the value of the mass flow rate ratio in each stage for  $0 \leq \Psi \leq 20$  kJ/kg dry air, and for  $N \leq 5$ .

## **Acknowledgments**

The authors would like to thank the King Fahd University of Petroleum and Minerals for funding the research reported in this paper through the Center for Clean Water and Clean Energy at MIT and KFUPM (Project # R4-CW-08).

## References

- [1] G. P. Narayan, M. H. Sharqawy, E. K. Summers, J. H. Lienhard V, S. M. Zubair, and M. A. Antar, “The potential of solar-driven humidification-dehumidification desalination for small-scale decentralized water production,” *Renewable and Sustainable Energy Reviews*, vol. 14, pp. 1187–1201, 2010.
- [2] G. P. Narayan, M. H. Sharqawy, J. H. Lienhard V, and S. M. Zubair, “Thermodynamic analysis of humidification dehumidification desalination cycles,” *Desalination and Water Treatment*, vol. 16, pp. 339–353, 2010.
- [3] K. Bourouni, M. Chaibi, and L. Tadrist, “Water desalination by humidification and dehumidification of air: state of the art,” *Desalination*, vol. 137, pp. 167–176, 2001.
- [4] K. H. Mistry, A. Mitsos, and J. H. Lienhard V, “Optimal operating conditions and configurations for humidification-dehumidification desalination cycles,” *International Journal of Thermal Sciences*, vol. 50, pp. 779–789, 2011.
- [5] J. A. Miller, “Numerical balancing in a humidification dehumidification desalination system,” Master’s thesis, Massachusetts Institute of Technology, 2011.
- [6] J. A. Miller and J. H. Lienhard V, “Impact of extraction on a humidification dehumidification desalination system,” *Desalination*, vol. 313, pp. 87 – 96, 2013.
- [7] G. P. Narayan, J. H. Lienhard V, and S. M. Zubair, “Entropy generation minimization of combined heat and mass transfer devices,” *International Journal of Thermal Sciences*, vol. 49, pp. 2057–66, 2010.
- [8] H. Müller-Holst, *Solar thermal desalination using the Multiple Effect Humidification (MEH) method in Solar Desalination for the 21st Century*, ch. 15, pp. 215–25. NATO Security through Science Series, Springer, Dordrecht, 2007.
- [9] H. Müller-Holst, *Mehrfacheffekt-Feuchtluftdestillation bei Umgebungsdruck - Verfahrensoptimierung und Anwendungen*. PhD thesis, Technische Universität Berlin, 2002.
- [10] M. Zamen, S. M. Soufari, and M. Amidpour, “Improvement of solar humidification-dehumidification desalination using multi-stage process,” *Chemical Engineering Transactions*, vol. 25, pp. 1091–1096, 2011.
- [11] S. Hou, “Two-stage solar multi-effect humidification dehumidification desalination process plotted from pinch analysis,” *Desalination*, vol. 222, p. 5728, 2008.

- [12] R. K. McGovern, G. P. Thiel, G. P. Narayan, S. M. Zubair, and J. H. Lienhard V, “Performance limits of zero and single extraction humidification-dehumidification desalination systems,” *Applied Energy*, vol. 102, pp. 1081 – 1090, 2012.
- [13] G. P. Thiel and J. H. Lienhard V, “Entropy generation in condensation in the presence of high concentrations of noncondensable gases,” *International Journal of Heat and Mass Transfer*, vol. 55, pp. 5133–5147, May 2012.
- [14] G. P. Narayan, K. M. Chehayeb, R. K. McGovern, G. P. Thiel, S. M. Zubair, and J. H. Lienhard V, “Thermodynamic balancing of the humidification dehumidification desalination system by mass extraction and injection,” *International Journal of Heat and Mass Transfer*, vol. 57, pp. 756 – 770, 2013.
- [15] G. P. Narayan, M. G. St. John, S. M. Zubair, and J. H. Lienhard V, “Thermal design of the humidification dehumidification desalination system: An experimental investigation,” *International Journal of Heat and Mass Transfer*, vol. 58, pp. 740 – 748, 2013.
- [16] G. P. Narayan, K. H. Mistry, M. H. Sharqawy, S. M. Zubair, and J. H. Lienhard V, “Energy effectiveness of simultaneous heat and mass exchange devices,” *Frontiers in Heat and Mass Transfer*, vol. 1, pp. 1–13, 2010.
- [17] D. Tondeur and E. Kvaalen, “Equipartition of entropy production. an optimality criterion for transfer and separation processes,” *Industrial & Engineering Chemistry Research*, vol. 26, pp. 50–56, 1987.
- [18] M. H. Sharqawy, J. H. Lienhard V, and S. M. Zubair, “Thermophysical properties of seawater: A review of existing correlations and data,” *Desalination and Water Treatment*, vol. 16, pp. 354–80, 2010.
- [19] S. Pruss and W. Wagner, “The iapws formulation 1995 for the thermodynamic properties of ordinary water substance for general and scientific use,” *Journal of Physical and Chemical Reference Data*, vol. 31, pp. 387–535, 2002.
- [20] R. W. Hyland and A. Wexler, “Formulations for the Thermodynamic Properties of Dry Air from 173.15 K to 473.15 K, and of Saturated Moist Air From 173.15 K to 372.15 K, at Pressures to 5 MPa,” *ASHRAE Transactions*, vol. Part 2A (RP-216), no. 2794, pp. 520–535, 1983b.
- [21] D. J. Wessel, *ASHRAE Fundamentals Handbook 2001 (SI Edition)*. American Society of Heating, Refrigerating, and Air-Conditioning Engineers, 2001.

- [22] E. W. Lemmon, M. L. Huber, and M. O. McLinden, “Standard reference database 23: Reference fluid thermodynamic and transport properties,” tech. rep., NIST - REFPROP, Version 8.0 (2007).



## Appendix: Detailed algorithm

[Fig. 15 about here.]

## List of Figures

1	Schematic diagram of a water-heated, closed-air, open-water HDH system consisting of $N + 1$ stages separated by $N$ air extractions from the humidifier to the dehumidifier. . . . .	28
2	Temperature-enthalpy profile of a balanced system without extractions/injections with $T_{feed} = 20$ °C, $T_{topbrine} = 80$ °C, and $\Psi_{hum} = \Psi_{deh} = 20$ kJ/kg dry air. . . . .	29
3	A control volume containing the heater, a section of the dehumidifier and the corresponding section of the humidifier. . . . .	30
4	Diagrams showing the control volumes used in the conservation of mass and energy equations in (a) the dehumidifier and (b) the humidifier. . . . .	31
5	Temperature-enthalpy profile of a balanced system with 3 extractions/injections, $T_{feed} = 20$ °C, $T_{topbrine} = 80$ °C, and $\Psi = 3$ kJ/kg dry air. . . . .	32
6	Effect of assuming fixed mass flow rate ratio on GOR for (a) $N = 0$ (b) $N = 1$	33
7	Optimal temperature of air extractions/injections for varying enthalpy pinch with $N \leq 5$ , $T_{feed} = 20$ °C, and $T_{topbrine} = 80$ °C. . . . .	34
8	Temperature of air extractions/injections at infinite area ( $\Psi = 0$ kJ/kg dry air) for varying number of extractions/injections, $N$ . . . . .	35
9	Variation of GOR with enthalpy pinch, $\Psi$ , and number of extractions/injections, $N$ . Boundary conditions: $T_{feed} = 20$ °C, $T_{topbrine} = 80$ °C. . . . .	36
10	Variation of RR with enthalpy pinch, $\Psi$ , and number of extractions/injections, $N$ . Boundary conditions: $T_{feed} = 20$ °C, $T_{topbrine} = 80$ °C. . . . .	37
11	Variation of Heat Duty with enthalpy pinch, $\Psi$ , and number of extractions/injections, $N$ . Boundary conditions: $T_{feed} = 20$ °C, $T_{topbrine} = 80$ °C. . . . .	38
12	Distribution of heat duty between the stages of the system at various numbers of extractions/injections, $N$ , at (a) $\Psi = 0$ kJ/kg dry air and (b) $\Psi = 2$ kJ/kg dry air. The percentage of the total heat duty in each stage is displayed in the corresponding column. . . . .	39
13	Optimal distribution of heat duty between the stages of the system at varying enthalpy pinch, $\Psi$ , and $N \leq 5$ . . . . .	40
14	Optimal mass flow rate ratio at each stage in the system for varying enthalpy pinch, $\Psi$ , and $N \leq 5$ . . . . .	41
15	Flowchart presenting the algorithm used in this study. . . . .	42

## Contents

<b>Nomenclature</b>	<b>2</b>
<b>1 Introduction</b>	<b>4</b>
1.1 Literature review . . . . .	5
1.2 Goals of the current study . . . . .	6
<b>2 Modeling</b>	<b>6</b>
2.1 Definition of a balanced system . . . . .	6
2.2 Conservation equations and solution method . . . . .	7
2.3 Assumptions and approximations . . . . .	11
2.4 Performance parameters . . . . .	12
2.5 Property packages . . . . .	13
<b>3 Results and Discussion</b>	<b>13</b>
3.1 Experimental validation . . . . .	13
3.2 Effect of assuming fixed mass flow rate ratio . . . . .	14
3.3 Temperature of the extracted streams . . . . .	15
3.4 Variation of GOR with enthalpy pinch and number of extractions . . . . .	16
3.5 Variation of Recovery Ratio with enthalpy pinch and number of extractions	18
3.6 Variation of heat duty with enthalpy pinch and number of extractions . . . . .	18
3.7 Division of heat duty between stages . . . . .	19
3.8 Optimal values for mass flow rate ratio for varying enthalpy pinch . . . . .	19
<b>4 Conclusions</b>	<b>20</b>
<b>Acknowledgments</b>	<b>21</b>

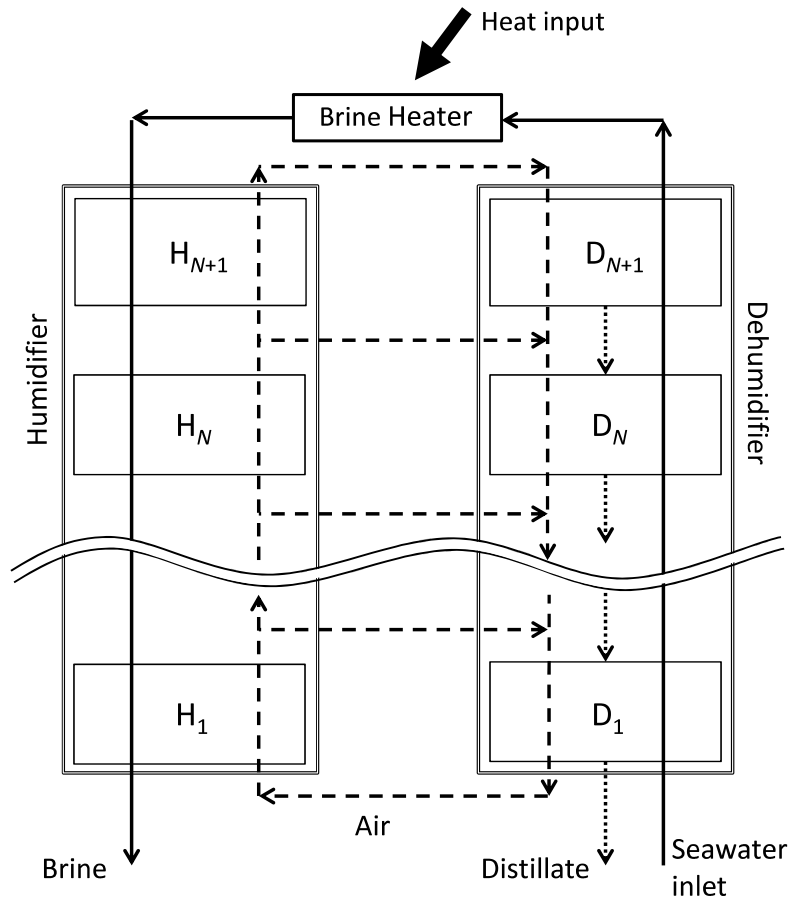


Fig. 1: Schematic diagram of a water-heated, closed-air, open-water HDH system consisting of  $N + 1$  stages separated by  $N$  air extractions from the humidifier to the dehumidifier.

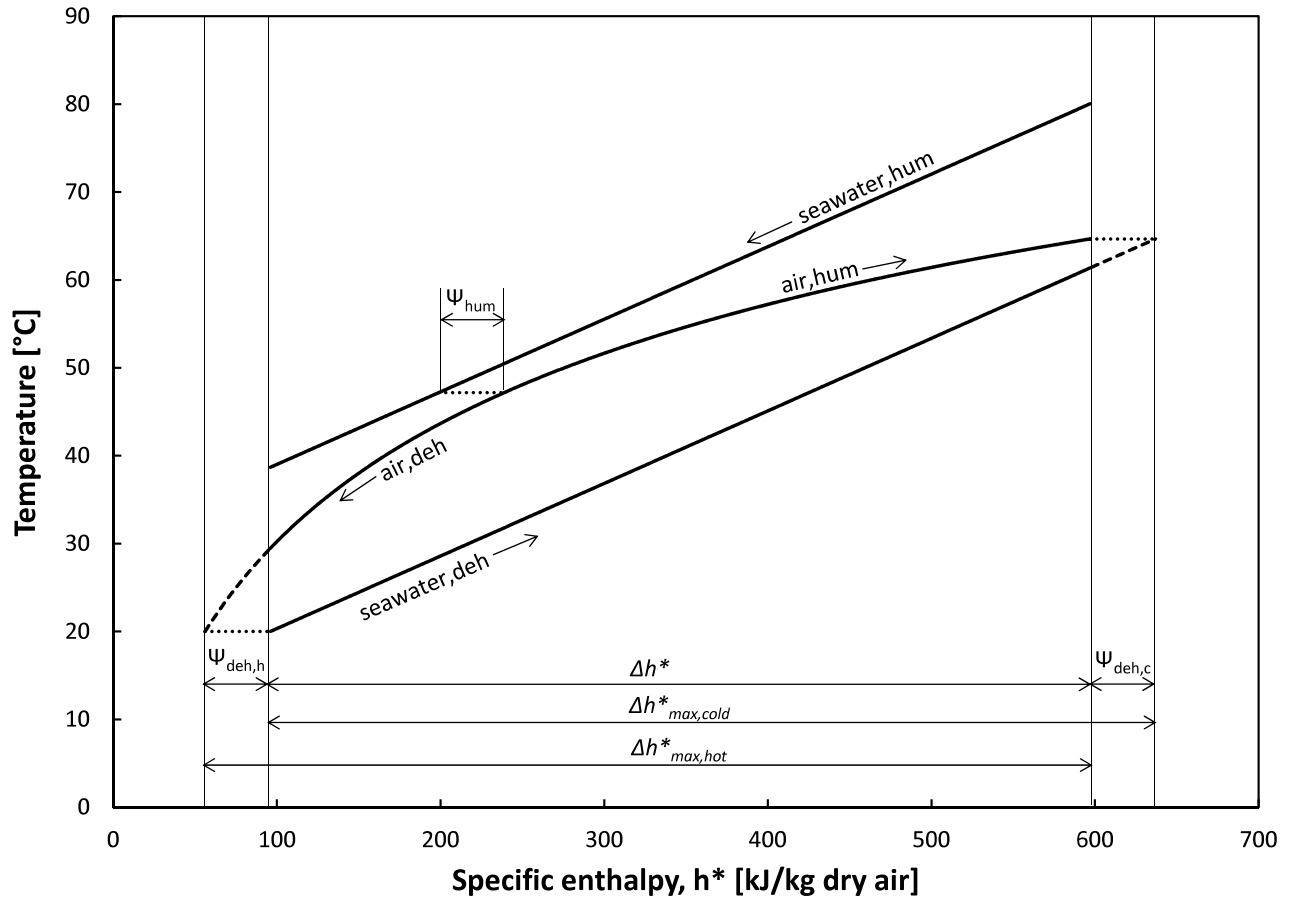


Fig. 2: Temperature-enthalpy profile of a balanced system without extractions/injections with  $T_{feed} = 20 \text{ }^\circ\text{C}$ ,  $T_{topbrine} = 80 \text{ }^\circ\text{C}$ , and  $\Psi_{hum} = \Psi_{deh} = 20 \text{ kJ/kg dry air}$ .

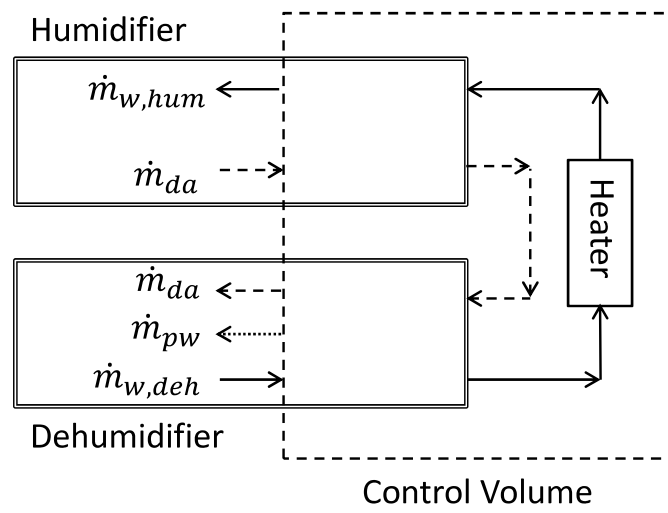
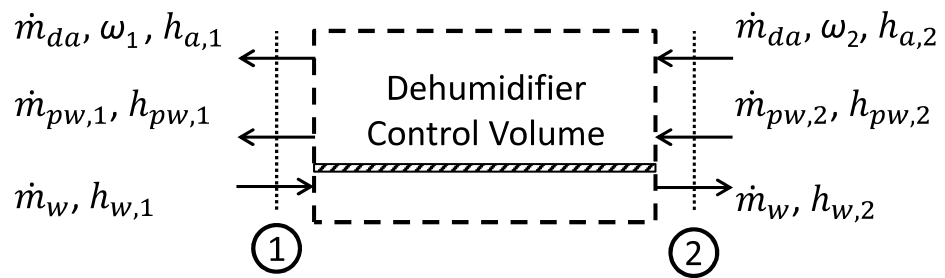


Fig. 3: A control volume containing the heater, a section of the dehumidifier and the corresponding section of the humidifier.



(a) Control volume in the dehumidifier



(b) Control volume in the humidifier

Fig. 4: Diagrams showing the control volumes used in the conservation of mass and energy equations in (a) the dehumidifier and (b) the humidifier.

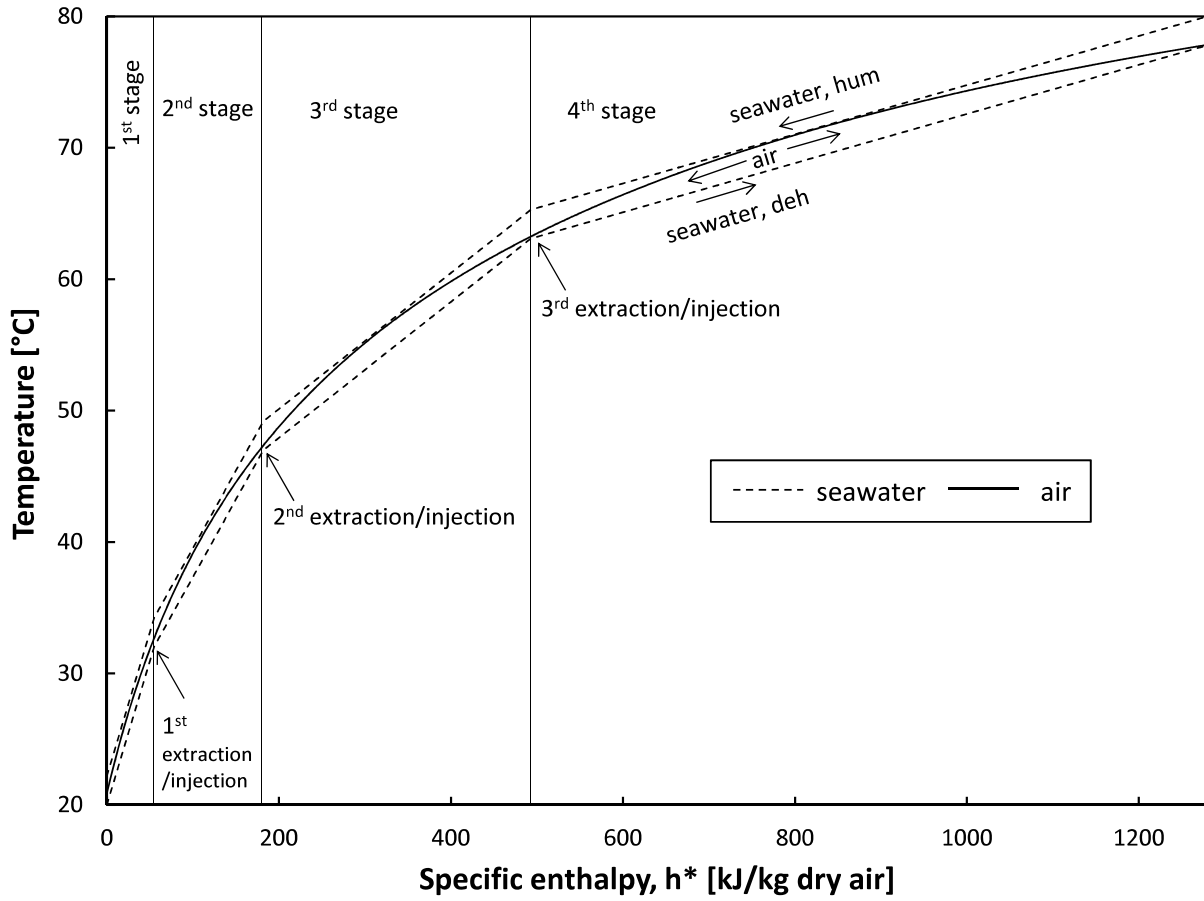
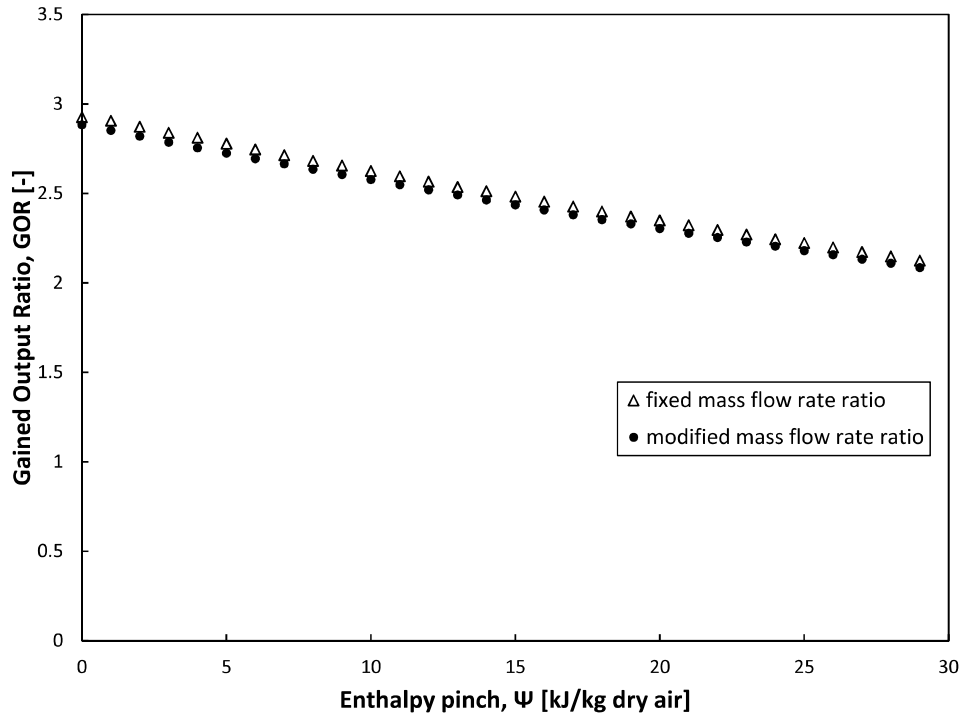
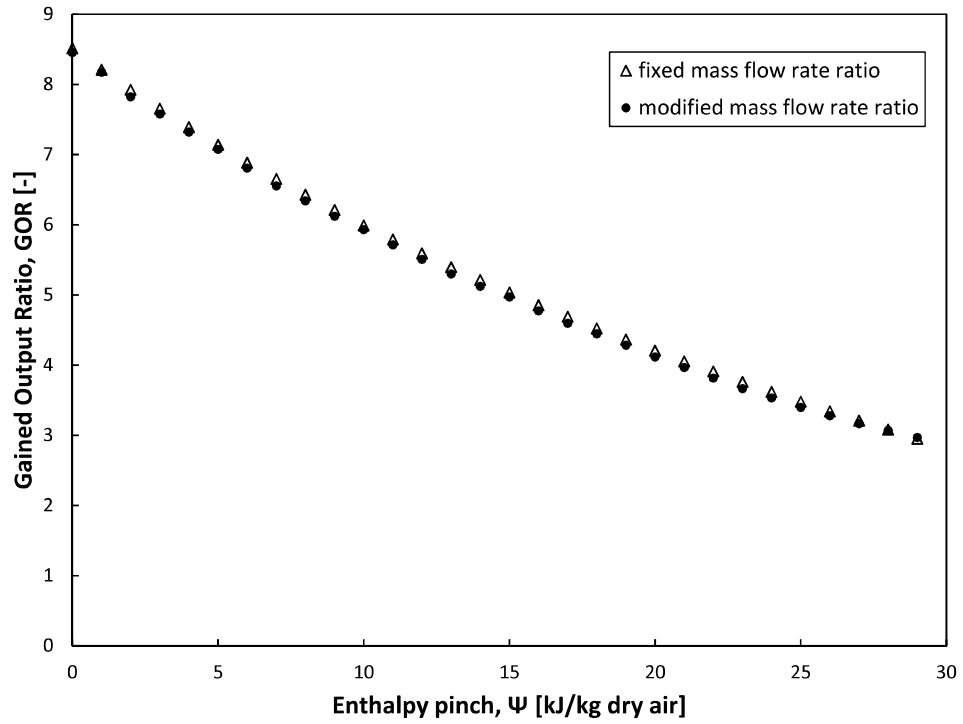


Fig. 5: Temperature-enthalpy profile of a balanced system with 3 extractions/injections,  $T_{feed} = 20 \text{ }^\circ\text{C}$ ,  $T_{topbrine} = 80 \text{ }^\circ\text{C}$ , and  $\Psi = 3 \text{ kJ/kg dry air}$ .





(a) Comparison of models with fixed and modified mass flow rate ratios for  $N = 0$



(b) Comparison of models with fixed and modified mass flow rate ratios for  $N = 1$

Fig. 6: Effect of assuming fixed mass flow rate ratio on GOR for (a)  $N = 0$  (b)  $N = 1$

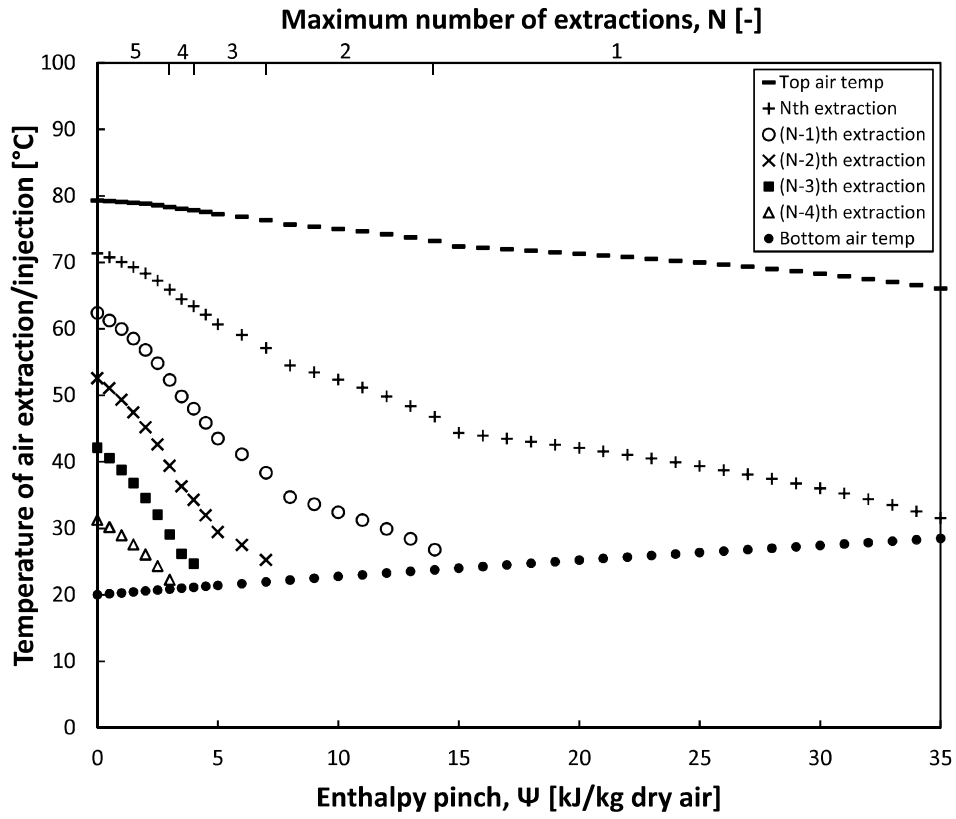


Fig. 7: Optimal temperature of air extractions/injections for varying enthalpy pinch with  $N \leq 5$ ,  $T_{feed} = 20$  °C, and  $T_{topbrine} = 80$  °C.

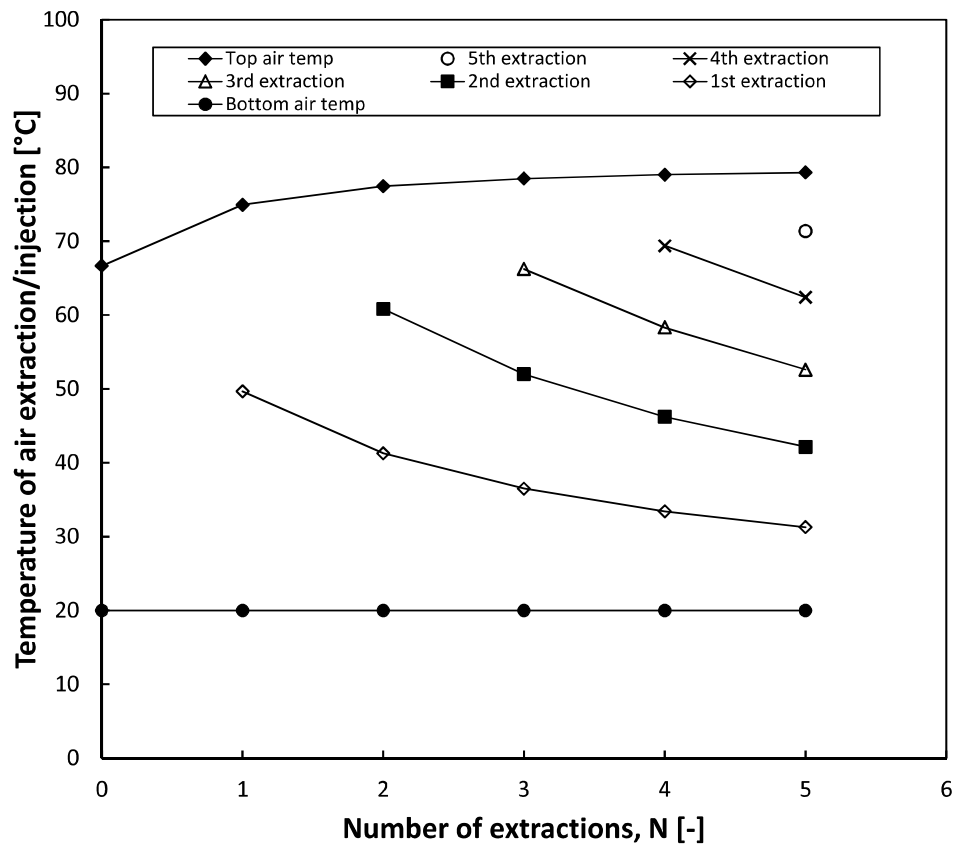


Fig. 8: Temperature of air extractions/injections at infinite area ( $\Psi = 0$  kJ/kg dry air) for varying number of extractions/injections,  $N$ .

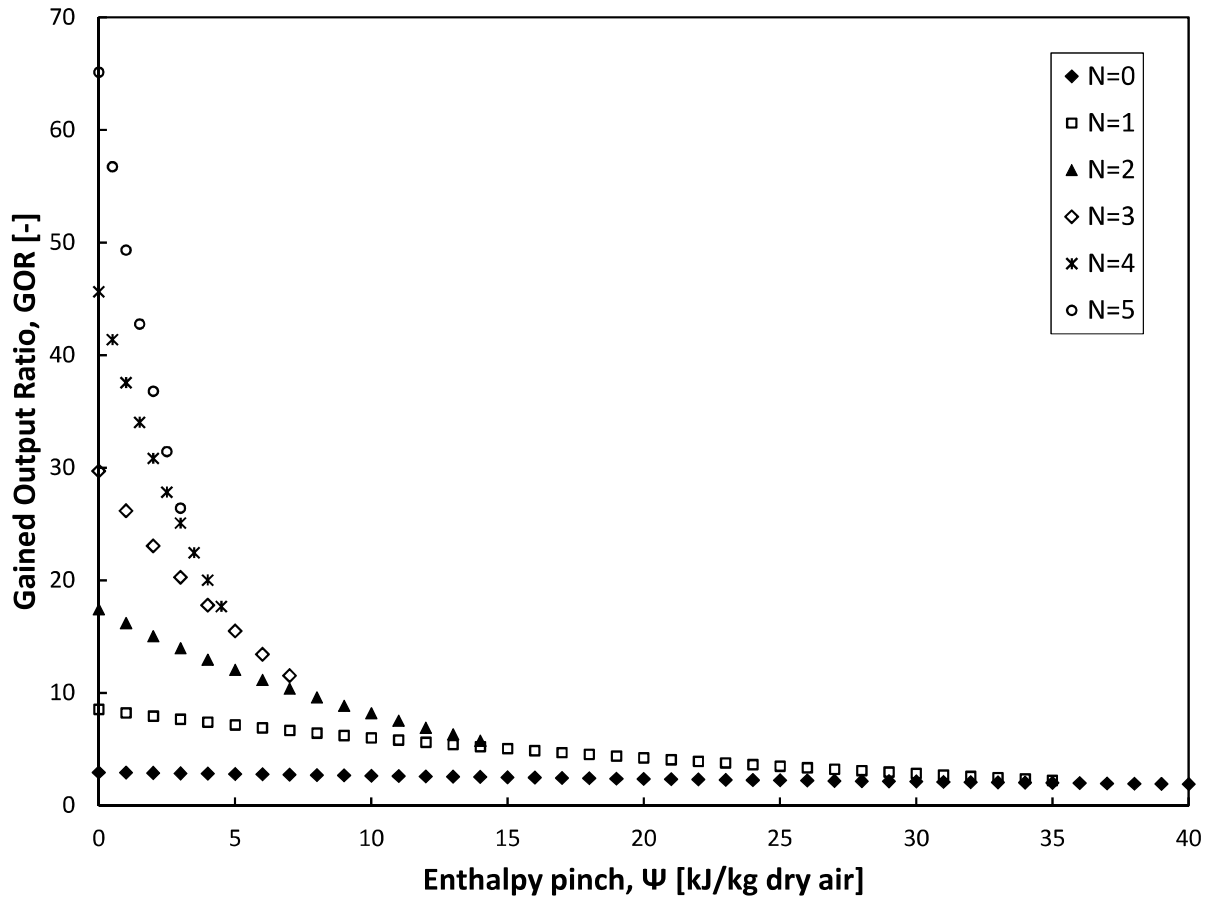


Fig. 9: Variation of GOR with enthalpy pinch,  $\Psi$ , and number of extractions/injections,  $N$ . Boundary conditions:  $T_{feed} = 20$  °C,  $T_{topbrine} = 80$  °C.

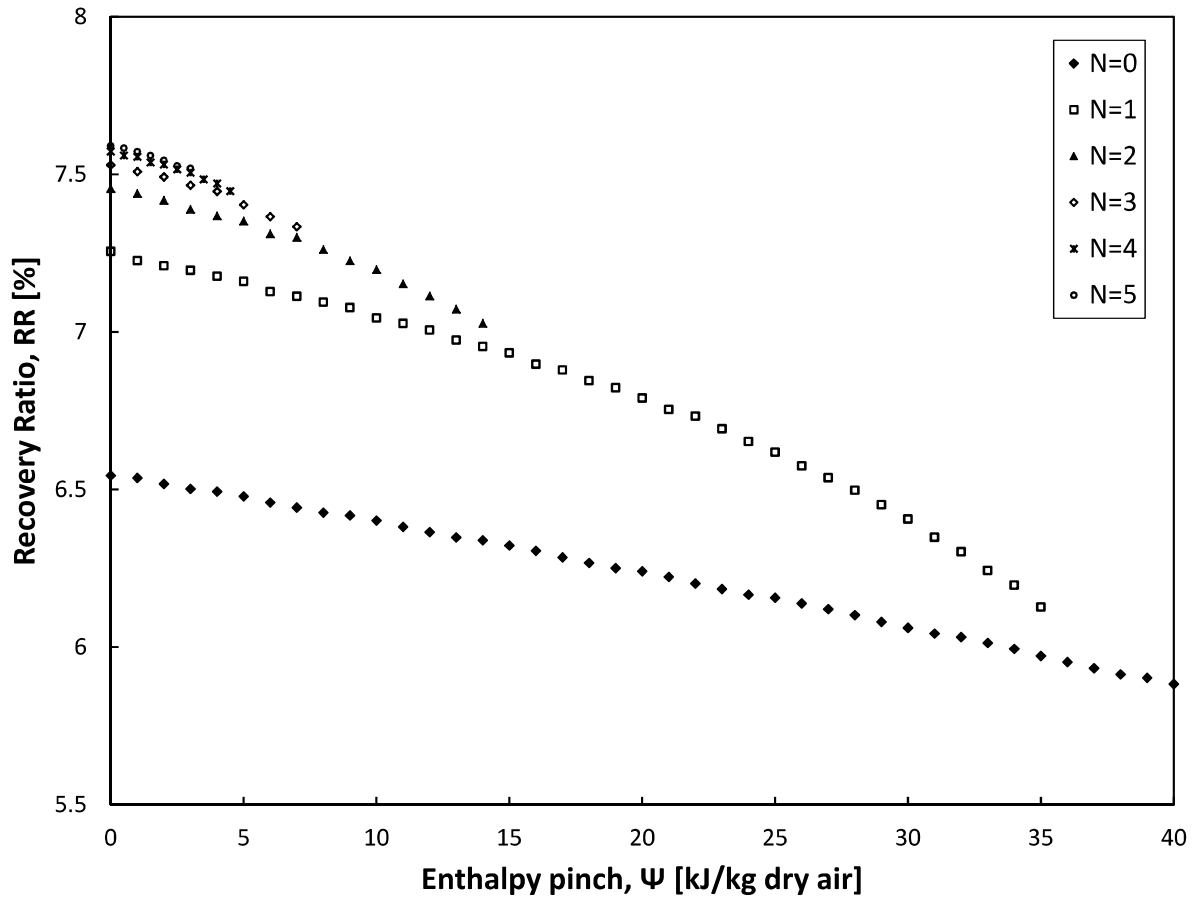


Fig. 10: Variation of RR with enthalpy pinch,  $\Psi$ , and number of extractions/injections,  $N$ . Boundary conditions:  $T_{feed} = 20$  °C,  $T_{topbrine} = 80$  °C.

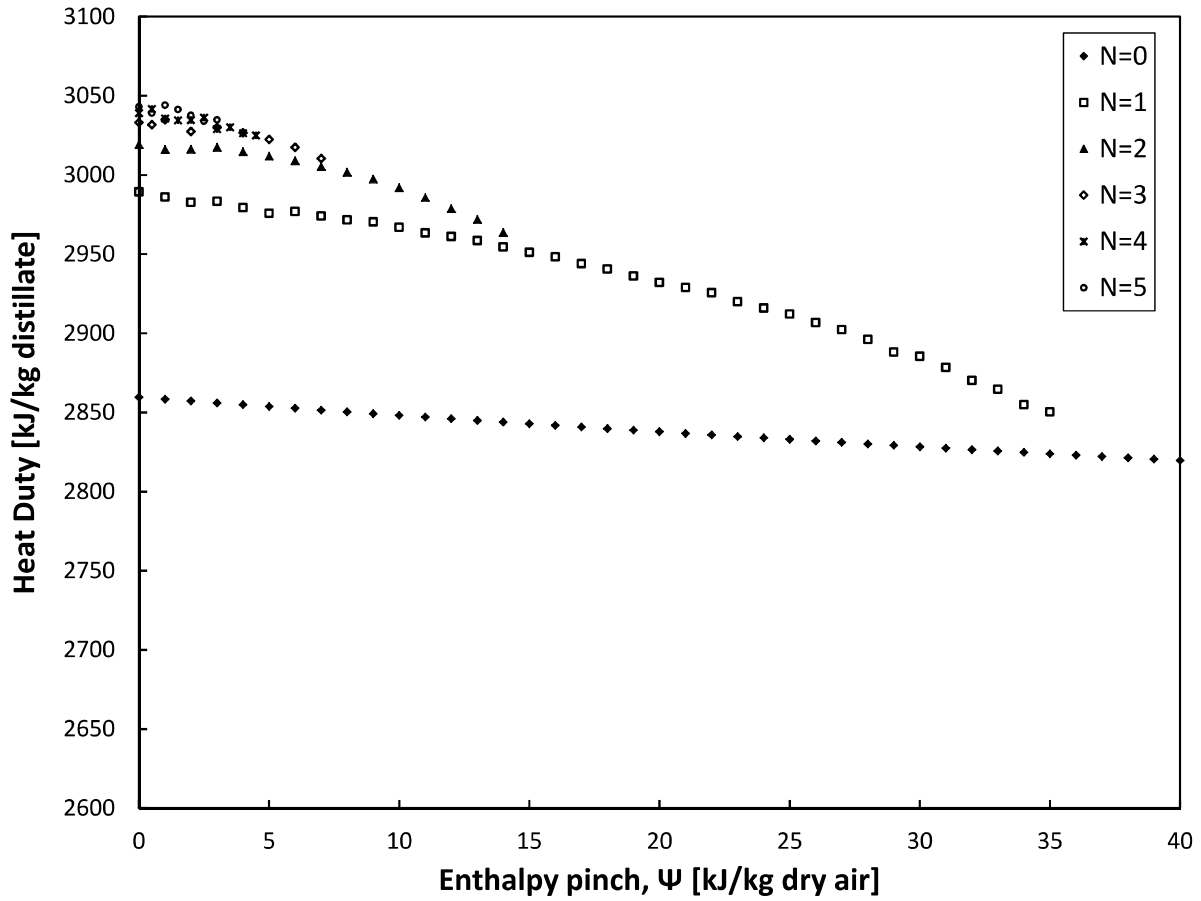
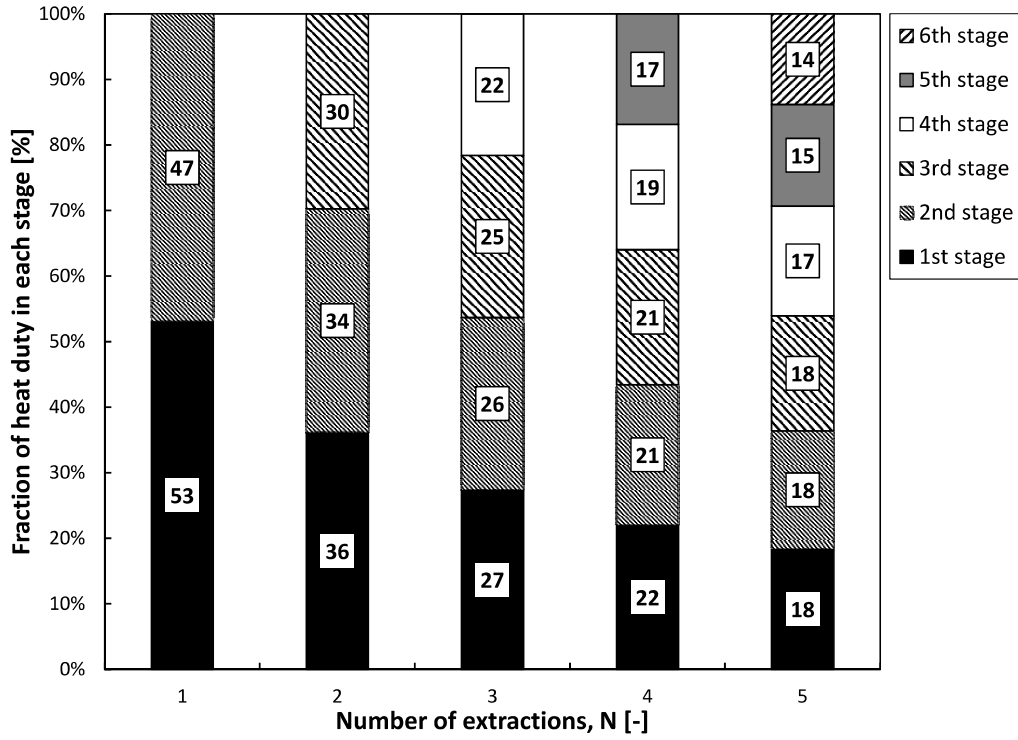
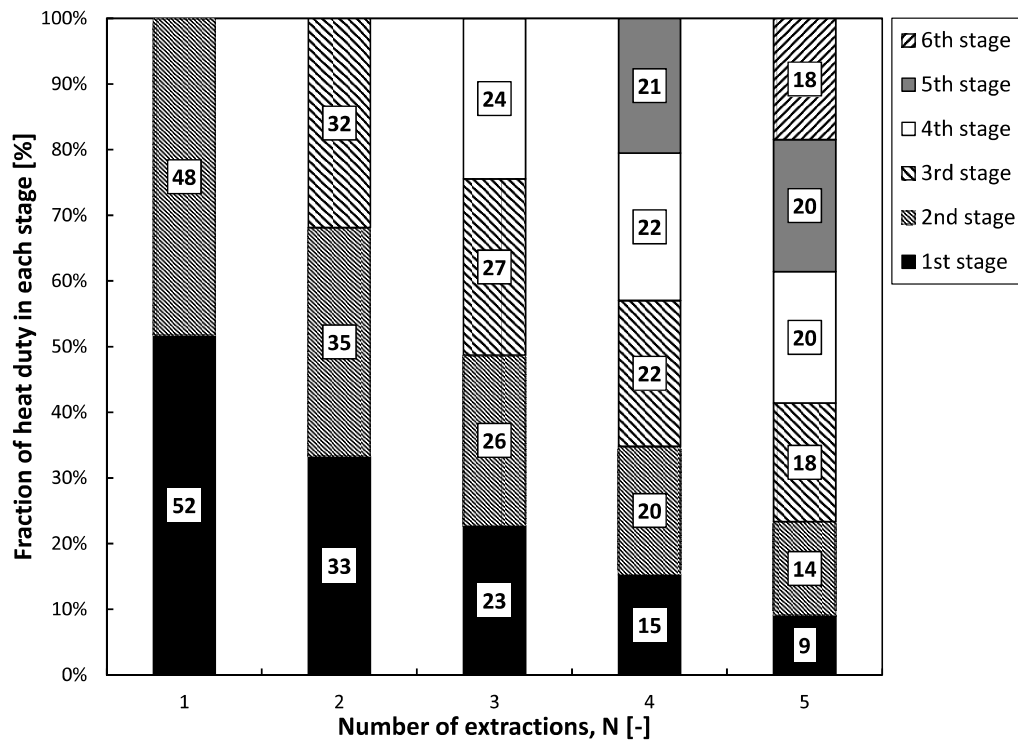


Fig. 11: Variation of Heat Duty with enthalpy pinch,  $\Psi$ , and number of extractions/injections,  $N$ . Boundary conditions:  $T_{feed} = 20$  °C,  $T_{topbrine} = 80$  °C.



(a)  $\Psi = 0$  kJ/kg dry air



(b)  $\Psi = 2$  kJ/kg dry air

Fig. 12: Distribution of heat duty between the stages of the system at various numbers of extractions/injections,  $N$ , at (a)  $\Psi = 0$  kJ/kg dry air and (b)  $\Psi = 2$  kJ/kg dry air. The percentage of the total heat duty in each stage is displayed in the corresponding column.

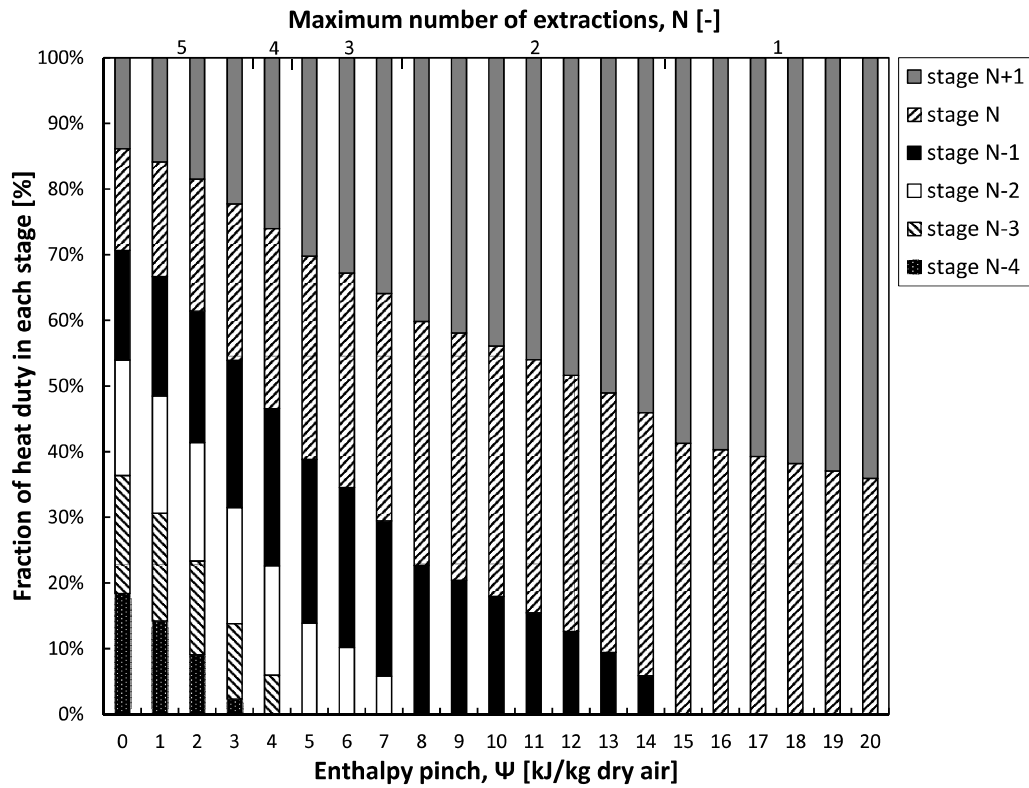


Fig. 13: Optimal distribution of heat duty between the stages of the system at varying enthalpy pinch,  $\Psi$ , and  $N \leq 5$ .



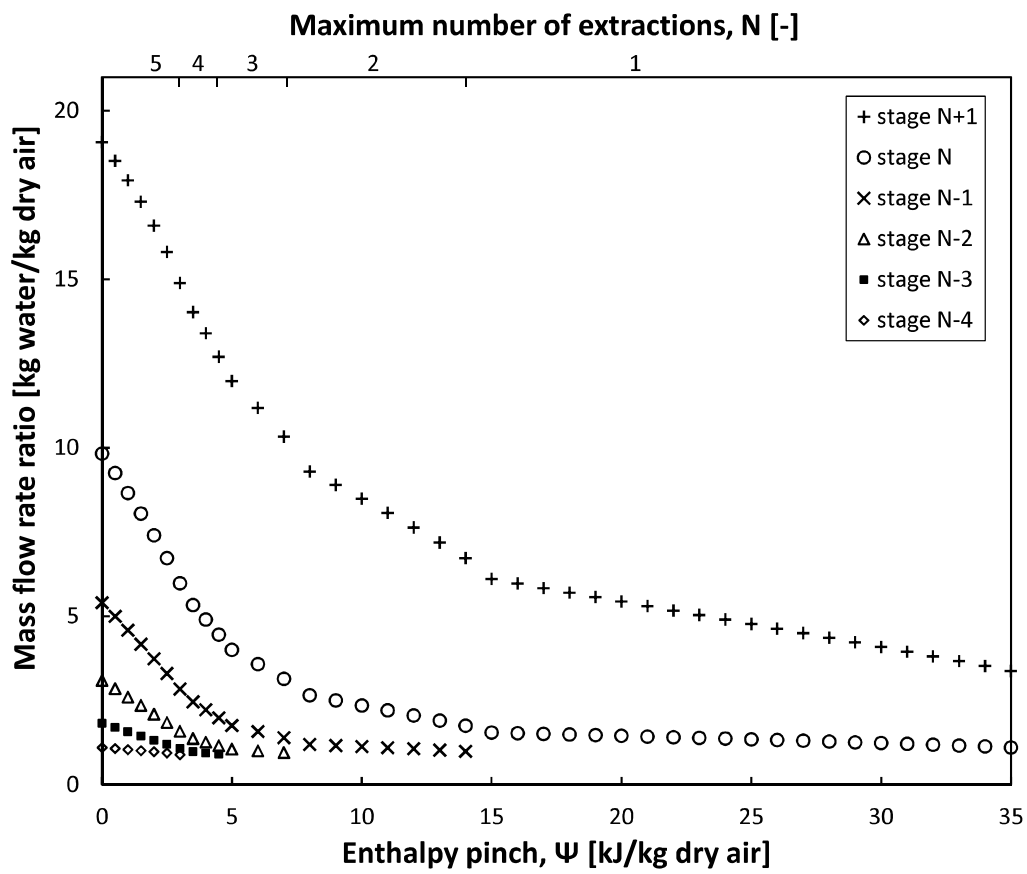


Fig. 14: Optimal mass flow rate ratio at each stage in the system for varying enthalpy pinch,  $\Psi$ , and  $N \leq 5$ .

